

Cite this: DOI: 10.1039/c2dt30512g

www.rsc.org/dalton

PAPER

Synthesis, structure, DNA-binding properties and antioxidant activity of silver(I) complexes containing V-shaped bis-benzimidazole ligands†

Huili Wu,* Jingkun Yuan, Ying Bai, Guolong Pan, Hua Wang, Jin Kong, Xuyang Fan and Hongmei Liu

Received 3rd March 2012, Accepted 11th May 2012

DOI: 10.1039/c2dt30512g

A V-shaped ligand bis(2-benzimidazol-2-ylmethyl)benzylamine **L**¹ with its two derivatives bis(*N*-methylbenzimidazol-2-ylmethyl)benzylamine **L**² and bis(*N*-benzylbenzimidazol-2-ylmethyl)benzylamine **L**³ have been prepared. Reaction of these shape-specific designed ligands with Ag(pic) (pic = picrate) afforded three novel complexes, namely, [Ag₂L¹]₂(pic)₂ **1**, [Ag₂L²]₂(pic)₂·2DMF **2** and [AgL³(pic)] **3**. The ligands and complexes were characterized on the basis of elemental analysis, UV-Vis, IR, NMR spectroscopy and X-ray crystallography. Complex **1** is a dinuclear metallacycle with a 2-fold rotational symmetry in which two *syn*-conformational **L**¹ ligands are connected by two linearly coordinated Ag(I) atoms. Due to the strong interaction between two adjacent Ag(I) atoms, the coordination mode of the central Ag(I) atom can be described as T-shaped. Complex **2** consists of a centrosymmetric dinuclear pore canal structure assembled from two nearly linearly coordinated Ag(I) atoms and two **L**² ligands. The structure of complex **3** adopts a four-coordinate environment for AgN₂O₂, with the counterion participating in an eight-shaped geometry. In order to explore the relationship between the structure and biological properties, the DNA-binding properties have been investigated by viscosity measurements, electronic absorption, and fluorescence. The results suggest that the ligands and complexes bind to DNA in an intercalation mode, and their binding affinities for DNA are also different. Moreover, the three Ag(I) complexes also exhibited potential antioxidant properties *in vitro* studies.

1. Introduction

Supramolecular chemistry of silver(I) coordination assemblies is a dynamic, thriving field which has drawn ever increasing research interest in recent decades.¹ Due to its flexible coordination sphere, the Ag(I) ion exhibits versatile coordination geometries, varying from linear to trigonal, tetragonal, square pyramidal, and octahedral, corresponding to coordination numbers 2 to 6, respectively. Such coordination flexibility contributes greatly to the structural diversity of Ag(I) polymers. So far, a large number of Ag(I) coordination polymers with diverse topologies and dimensionalities [one-, two- or three-dimensions (1D, 2D, or 3D)²] have been constructed. As more and more silver complexes with novel topological structures have been synthesized, the investigation into the relationship between the structure and properties, especially biological properties, is becoming another popular and promising field.³

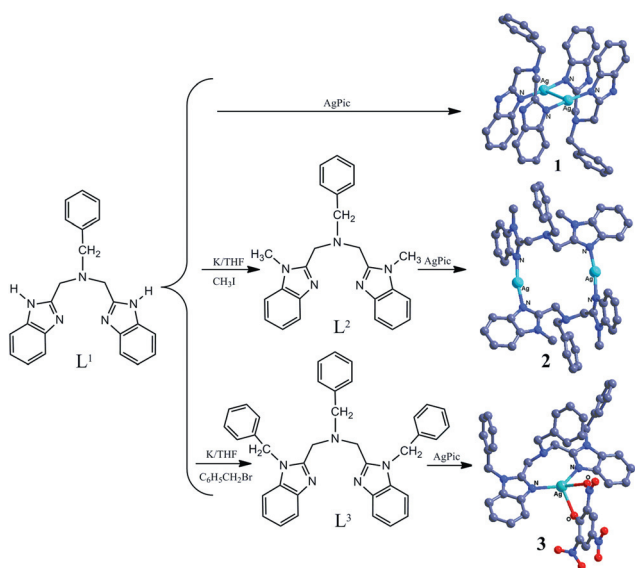
Nitrogen ligands have been extensively used in coordination chemistry,⁴ especially to obtain derivatives able to mimic

structural, spectroscopic and catalytic features of active sites of metallo-enzymes.⁵ As a typical heterocyclic ligand, interest in exploring benzimidazole derivatives and their metal complexes has continually increased since the recognition that many of these materials may serve as models which mimic both the structure and reactivity of metal ion sites in complex biological systems and possess a broad spectrum of biological activity.^{4,6} Due to their intriguing varying architectures and their important properties that span from luminescence to biological activities,⁷ benzimidazoles and their derivatives, including the designed ligands which are benzimidazole-based, also exhibit wide-ranging antiviral activities,⁸ photochemical and photophysical properties,⁹ versatile coordination modes, and the potential to form supramolecular aggregates through $\pi\cdots\pi$ stacking interactions and hydrogen bonding.¹⁰

In the framework of our research project, mainly focusing on studying transition metal complexes containing benzimidazole derivatives, we have investigated the DNA binding ability of such complexes in our previous publications.¹¹ In this paper, the synthesis, characterization and DNA-binding activities of the silver complexes with three different V-shape ligands are presented. According to relevant reports in the literature,¹² some similar transition metal complexes can exhibit antioxidant activity. We therefore also conducted an investigation into the hydroxyl radical scavenging properties of these complexes.

School of Chemical and Biological Engineering, Lanzhou Jiaotong University, Lanzhou 730070, People's Republic of China.
E-mail: wuhuilu@163.com; Fax: +(86)931-4956512;
Tel: +(86)13893117544

† Electronic supplementary information (ESI) available. CCDC 831425, 831426 and 831427. For ESI and crystallographic data in CIF or other electronic format see DOI: 10.1039/c2dt30512g



Scheme 1 Synthesis of ligands and complexes 1–3.

2. Results and discussion

Synthetic routes of ligands and Ag(I) complexes are shown in Scheme 1. L^1 has been reported in previous literature. Ligands L^2 and L^3 were synthesized on the basis of ligand L^1 . By contrast with the Ag(I) complexes, the three ligands are very stable in air. Both ligands and complexes are remarkably soluble in polar aprotic solvents such as DMF, DMSO and MeCN; slightly soluble in ethanol, methanol, ethyl acetate and chloroform; insoluble in water, Et₂O, petroleum ether. The molar conductivities in DMF solution indicate that the ligands are nonelectrolyte compounds, while the electrolytic conductivity of complexes **1** and **2** show that they are 1 : 1 electrolytes in DMF.¹³ In theory, complex **3** should be a neutral compound, but the conductivity shows that there may be partial ionization of the discrete $[AgL^3(pic)]$ in DMF.

2.1. IR and electronic spectra

The IR spectra of complex **1** are closely related to that of the free ligand L^1 . One of the most diagnostic changes occurs in the region between 1650 and 1250 cm⁻¹. The spectrum of L^1 shows a strong band at 1438 cm⁻¹ and weak bands at 1622 cm⁻¹. By analogy with the assigned bands of imidazole, the two bands are attributed to the $\nu(C=N)$ and $\nu(C=C)$ frequencies of the benzimidazole group, respectively.¹⁴ The location of the two bands was slightly shifted for complex **1**; the band at 1438 cm⁻¹ is shifted to 1454 cm⁻¹, which can be attributed to the coordination of the benzimidazole nitrogen to the metal center atom.¹⁵ Similar shifts also appear in complexes **2** and **3**, which gives the same conclusion. Moreover, information regarding the possible bonding modes of the picrate and benzimidazole rings may also be obtained from the IR spectra.¹¹

DMF solutions of ligands and Ag(I) complexes show, as expected, almost identical UV spectra. The UV bands of L^1 (278, 284 nm) are only marginally redshifted about 3 nm for complex **1**, which is evidence of C=N coordination to the metal center. These bands are assigned to $n \rightarrow \pi^*$ and $\pi \rightarrow \pi^*$

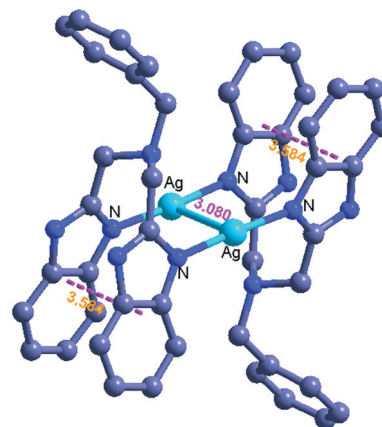


Fig. 1 Ball and stick representation of the $[Ag_2L^1_2]^{2+}$ cation.

(imidazole) transitions.¹¹ Analogously, the UV bands of L^2 (279, 287 nm), L^3 (279, 287 nm) are also marginally redshifted about 2–3 nm in complexes **2** and **3**. This phenomenon also shows that C=N is involved in coordination to the metal center. The picrate bands (observed at 381 nm in the complexes) are assigned to $n \rightarrow \pi^*$ transitions.¹¹

2.2. X-ray structures of the complexes

Crystal structure of complex 1. The crystal structure of complex **1** consists of a binuclear $[Ag_2L^1_2]^{2+}$ motif and two picrate anions per formula unit. Two ligands are arranged in a face-to-face *syn*-conformation to coordinate with two Ag(I) atoms from opposite directions, generating a locally linear geometry around the metal atoms. However, the coordination geometry around Ag(I) should be best described as T-shaped owing to the strong interaction between the two Ag(I) atoms themselves ($d_{Ag...Ag} = 3.080(0)$ Å),¹⁶ as shown in Fig. 1. The $[Ag_2L^1_2]^{2+}$ cation has high symmetry. A mirror plane m , containing two nitrogen atoms of the benzylamine, divides the ligand into two equivalent parts, while a C_2 axis passes through the two Ag(I) atoms. Thus, a crystallographically imposed $2/m$ symmetry is located at the center of the cluster and generates the entire molecule from the asymmetric unit, containing only half of a ligand and an Ag(I) atom. The two benzimidazole rings belonging to the same ligands are nearly parallel to each other (end-to-end, dihedral angle $\tau = 15.13^\circ$), resulting in intramolecular $\pi \cdots \pi$ interactions (centroid-to-centroid distance, $d = 3.584$ Å).¹⁷

As shown in Fig. 2, two benzene rings from two contiguous $[Ag_2L^1_2]^{2+}$ located in the same line are in a parallel position, so the geometry of the complex ion is propagated into an infinite 1-D chain *via* inter-ligand $\pi \cdots \pi$ interactions (i, $d = 3.864(0)$ Å). Two adjacent picrate anions are inlaid in the coordination cations as a sandwich and are concatenated by the $\pi \cdots \pi$ interactions (ii, $d = 3.462(0)$ Å). Such arrangement allows NH and other groups to contribute to formation of hydrogen bonds, which make the crystal structure more stable. Neighboring chains are connected by N–H \cdots O and C–H \cdots O hydrogen bonds, thus generating an infinite 2-D layer.

Crystal structure of 2. For complex **2**, the structure consists of a dinuclear $[Ag_2L^2_2]^{2+}$, two picrate anions and two dimethyl

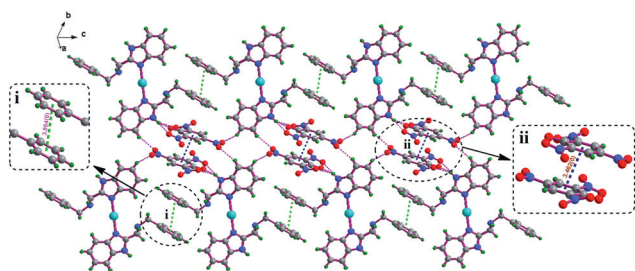


Fig. 2 2-D layer formed via $\pi\cdots\pi$ interactions and H bonds in **1** (different interactions are distinguished by different colors).

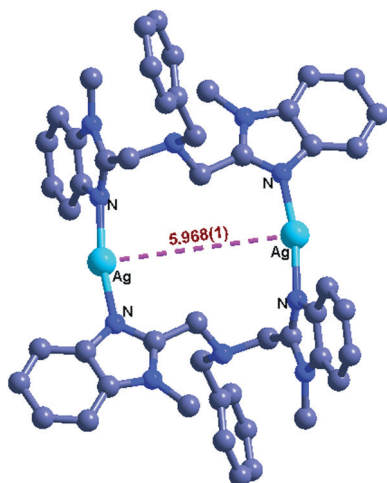


Fig. 3 Ball and stick representation of the $[\text{Ag}_2\text{L}_2]^{2+}$ cation.

formamide (DMF) molecules in a unit. As Fig. 3 shows, two Ag(i) atoms are bridged by two L^2 ligands, arranged in an end-to-end to fashion, forming an $[\text{Ag}_2\text{L}_2]^{2+}$ metallacycle, in which every Ag(i) atom is almost linearly coordinated by two N atoms from two benzimidazole rings belonging to the different ligands, and the distance between the two Ag(i) centres is 5.968(1) Å, precluding any bonding interaction. The line connected between two Ag(i) atoms has a role of 2-fold axis in the dinuclear $[\text{Ag}_2\text{L}_2]^{2+}$.

In complex **2**, adjacent benzimidazole rings and picrates are concatenated by the $\pi\cdots\pi$ interactions ($d = 3.480(0)$ Å), as shown in Fig. 4. In addition, hydrogen bonds (C–H \cdots O) also contribute to the stability of the structure. The formation of the 2-D infinite layer in the bc plane undoubtedly owes to such arrangement.

Due to the unique spatial distribution and interactions, the central metal atoms present a wavy arrangement along the c -axis, as depicted in Fig. 5, which has been reported rarely in previous studies.

Additionally, the $[\text{Ag}_2\text{L}_2]^{2+}$ cation makes up a centrosymmetric dinuclear pore canal structure via two ligands which are coordinated to two Ag(i) atoms. The maximum and minimum distances of the pore are 5.968(1) and 4.514(5) Å, respectively, as shown in Fig. 6. From the stacking of complex **2**, many parallel channels were constructed, which afforded an opportunity to investigate the potential in molecular recognition and gas absorption. Due to the existence of the hydrogen bonds and the $\pi\cdots\pi$

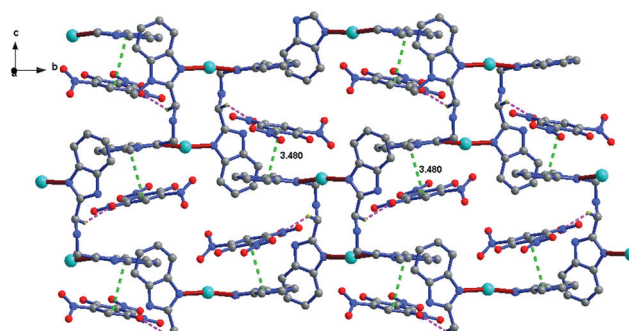


Fig. 4 2-D layer generated by the $\pi\cdots\pi$ interactions and weak O \cdots H–C hydrogen bonding in the bc plane in **2** (for clarity, some atoms were omitted).

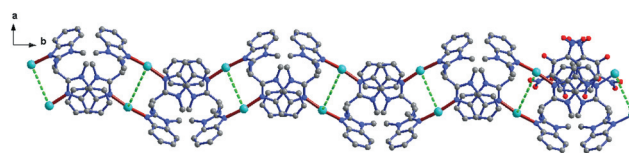


Fig. 5 A view of the waves configuration of the $[\text{Ag}_2\text{L}_2]^{2+}$ cation in the ab plane in **2** (for clarity, only two picrate molecules are shown).

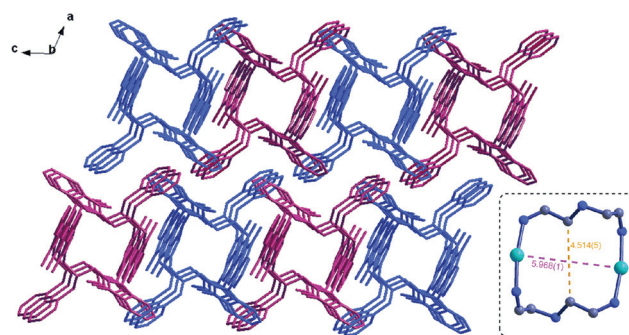


Fig. 6 3-D network of the $[\text{Ag}_2\text{L}_2]^{2+}$ cation.

stacking interactions, an infinite 3-D network was created in complex **2**.

Crystal structure of 3. Compared with complexes **1** and **2**, the coordination geometry of Ag(i) adopts a 4-coordinating configuration. For complex **3** (Fig. 7a), the structure consists of a central metal Ag(i) atom, a L^3 and a picrate. The Ag(i) center is a four-coordinated distorted tetrahedron, in which two oxygen atoms from picrate and two nitrogen atoms from L^3 participate in coordination (Fig. 7c). Owing to this coordination geometry, an 8-membered ring and a 6-membered ring were constructed, which are connected through the Ag(i) center and displaying an eight-shaped geometry (Fig. 7b).

In complexes **1** and **2**, the interactions, including $\pi\cdots\pi$ interactions and hydrogen bonds, contribute to formation of a 2-D infinite sheet. Similarly, as depicted in Fig. 8, there are two kinds of $\pi\cdots\pi$ interactions in complex **3**: (i) Between two adjacent picrates from different units, $d = 3.800(4)$ Å. (ii) Between two benzimidazole rings located in the face-to-face position, $d = 3.842(2)$ Å. It is precisely such layout that makes the formation of an infinite 1-D zigzag chain.

By comparing the ligands and complexes above-mentioned, the reason that the three Ag(I) complexes showed different spatial geometric structure can be attributed to the different steric hindrance and distortion of the ligands, which can be explained by the introduction of the different substituent groups.

2.3. DNA binding properties

Viscosity titration measurements. Hydrodynamic measurements that are sensitive to the length change (*i.e.*, viscosity and

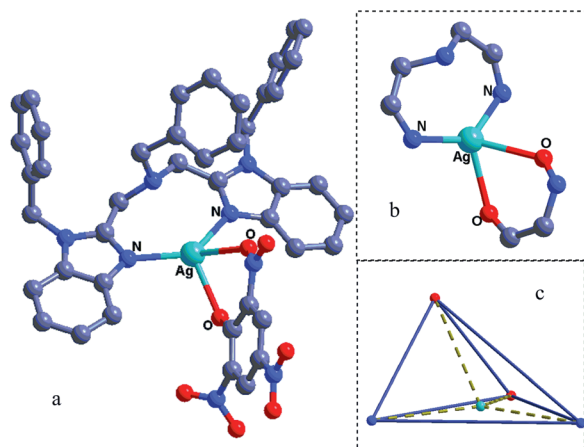


Fig. 7 Ball and stick representation of complex 3.

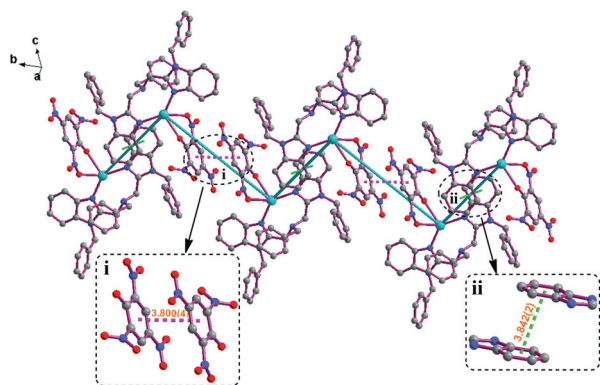


Fig. 8 1-D zigzag chain formed *via* the $\pi\cdots\pi$ interactions in 3.

sedimentation) are regarded as the least ambiguous and the most critical tests of the interaction model in solution in the absence of crystallographic structural data.¹⁸ Viscosity titration measurements were carried out to clarify the interaction modes between the investigated compounds and CT-DNA. Intercalation involves the insertion of a planar molecule between DNA base pairs, which results in a decrease in the DNA helical twist and lengthening of the DNA, therefore intercalators cause the unwinding and lengthening of DNA helix as base pairs become separated to accommodate the binding compound.¹⁹ Whereas, agents bound to DNA through groove binding do not alter the relative viscosity of DNA, and agents electrostatically bound to DNA will bend or kink the DNA helix, reducing its effective length and its viscosity, concomitantly.^{18a,e,20} The effects of ligands and Ag(I) complexes on the viscosities of CT-DNA are shown in Fig. 9. With the ratios of the investigated ligands to DNA increasing, the relative viscosities of DNA also show an upward trend, and almost at the same magnitude of change, indicating that there exist intercalations between all the ligands with DNA helix. However, for the three complexes, though the results indicated they all bind to DNA *via* an intercalation binding mode, the difference in magnitude of change suggested the extents of the unwinding and lengthening of DNA helix and DNA binding affinities follow the order: 2 > 3 > 1.

It is well known that varying the substituting group or substituent position in the intercalative ligand can create some interesting differences in the space configuration and the electron density distribution of transition metal complexes, which will result in some differences in spectral properties and the DNA-binding behaviors of the complexes and will be helpful to more clearly understand the binding mechanism of transition metal complexes to DNA.²¹ Based on the above results, we found that the affinity for DNA is stronger in case of Ag(I) complexes when compared with the ligands. For this difference, we attributed three possible reasons. (i) By comparison of the molecular structure of the ligands and Ag(I) complexes, we find the greater number of coplanar aromatic rings, which facilitate intercalation to the base pairs of double helical DNA, may lead to higher affinity for DNA.^{11/sg} (ii) The charge transfer of coordinated ligands caused by the coordination of the central atom lead to the decrease of the charge density of the plane conjugate system, which is conducive to insertion. (iii) This difference in their DNA binding ability also could be attributed to the presence of an electron deficient center in the charged Ag(I) complexes

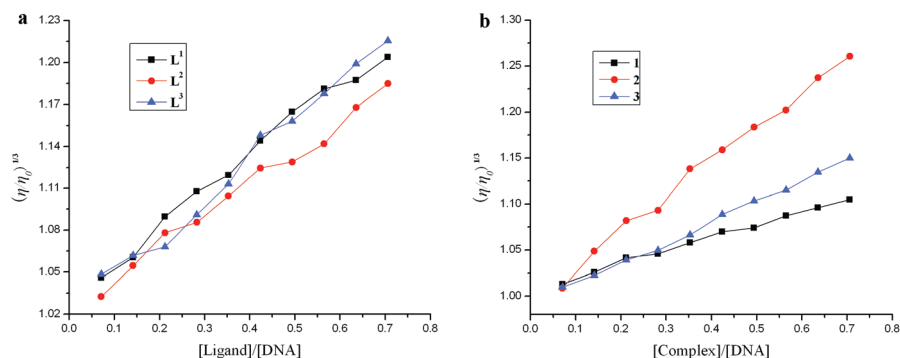


Fig. 9 Effect of increasing amounts of (a) ligands and (b) Ag(I) complexes on the relative viscosity of CT-DNA at 25.0 ± 0.1 °C.

where an additional interaction between the complex and phosphate-rich DNA backbone may occur.²²

In addition, the reason for the difference in the binding strength for three Ag(I) complexes can be attributed to the difference in steric hindrance and electron density, which are both caused by the introduction of substituents and geometric structure.

Electronic absorption titration. Absorption titration can monitor the interaction of a compound with DNA. The obvious hypochromism and bathochromism shift are usually characterized by the noncovalent intercalative binding of a compound to the DNA helix, due to the strong stacking interaction between the aromatic chromophore of the compound and base pairs of DNA.^{18,23} However, the intercalation between a compound and DNA helix cannot be excluded only by no or small redshift of UV-vis absorption bands. In fact, some groove binders of the Hoechst 33258 family can also present redshifts or even blueshifts of absorption bands when they bind to the DNA helix by groove binding modes, especially for multiple binders.²⁴

The absorption spectra of ligands and complexes in the absence and presence of CT-DNA (at a constant concentration of compounds) are given in Fig. 10a–c. As can be seen from Fig. 10a–c, the ligands and complexes exhibit intense absorption bands at 274–277 nm assigned to $\pi \rightarrow \pi^*$ transition of the benzimidazole, and addition of increasing amounts of CT-DNA results in hypochromism and bathochromic shift in the UV-vis spectra of the compounds. In the present case, with addition of DNA, three ligands exhibit hypochromism of about 28.5%, 17.3% and 25.6% accompanied by bathochromism of about a 1–2 nm shift in the absorption maxima. Corresponding complexes exhibit hypochromism of about 38.5%, 46.8% and 57.0%, and also accompanied by bathochromism of about a 1–2 nm shift in the absorption maxima. The hypochromism suggested that the compounds interact with CT-DNA.²⁵

To compare quantitatively the affinity of ligands and Ag(I) complexes toward DNA, the intrinsic binding constants K_b were calculated by plotting the changes in the absorbance of the complex upon incremental addition of increasing concentration of DNA. The K_b values of ligands **L**¹–**L**³ were $1.07 \times 10^3 \text{ M}^{-1}$ ($R = 0.97$ for 16 points), $7.41 \times 10^3 \text{ M}^{-1}$ ($R = 0.99$ for 13 points) and $1.78 \times 10^3 \text{ M}^{-1}$ ($R = 0.99$ for 16 points), respectively. That of complexes **1**–**3** were $4.85 \times 10^4 \text{ M}^{-1}$ ($R = 0.97$ for 8 points), $6.25 \times 10^5 \text{ M}^{-1}$ ($R = 0.99$ for 16 points) and $3.24 \times 10^5 \text{ M}^{-1}$ ($R = 0.99$ for 16 points), respectively. Therefore, compared with the classic DNA-intercalative reagents, such as ethidium bromide (EB), acridine orange (AO) and methylene blue (MB),²⁶ the binding constants (K_b) of the Ag(I) complexes can suggest that three Ag(I) complexes most probably bind to DNA in an intercalation mode. The magnitude of the K_b value is parallel to the intercalative strength and the affinity of a compound binding to DNA.²⁷ Hence, the magnitude of K_b values can prove that the three ligands have similar DNA-binding ability. Besides, it also indicates that the binding affinities of the Ag(I) complexes follow the order: **2** > **3** > **1**, which are in good agreement with the orders of viscosity titration results.

Competitive binding with ethidium bromide. The ability of a complex to change the fluorescence intensity of ethidium

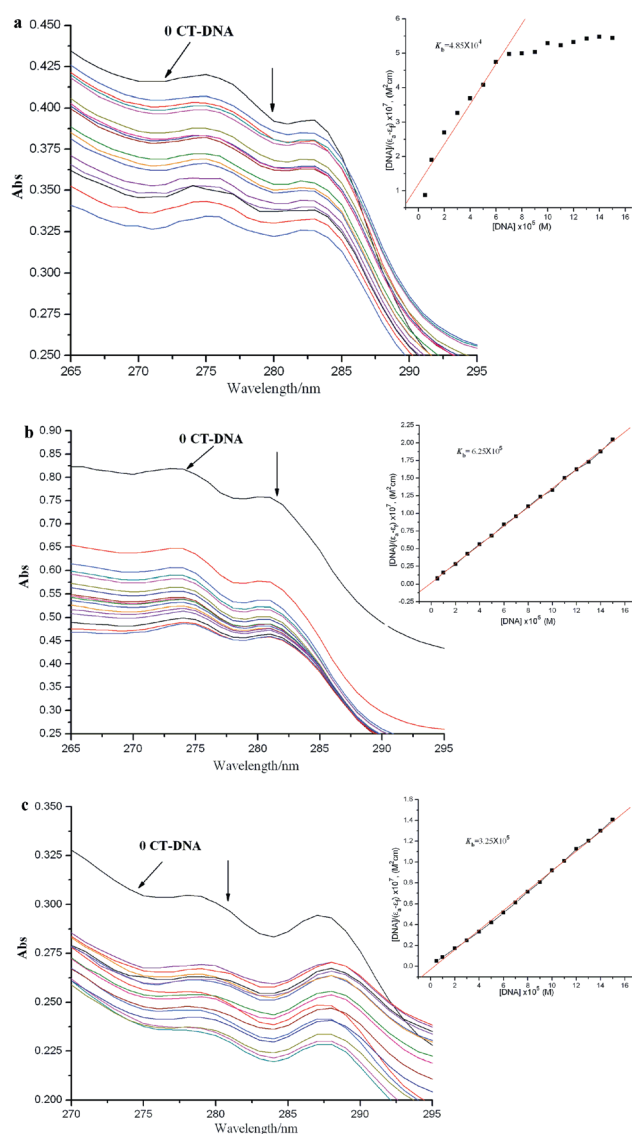


Fig. 10 Absorption spectra of compounds in the presence of CT-DNA (the DNA absorption was subtracted). The concentration of complexes (a) **1**, (b) **2**, and (c) **3** was kept constant at $3 \times 10^{-5} \text{ M}^{-1}$. Arrows show the absorbance changes upon increasing DNA concentration. Inset: plots of $[\text{DNA}]/(\epsilon_a - \epsilon_f)$ versus the titration of DNA with compound; ■, experimental data points; solid line, linear fitting of the data.

bromide (EB) in its EB–DNA adduct has been reported as a standard intercalating agent of DNA and it is a reliable tool to measure the affinity of the complex for DNA, irrespective of the binding modes. Therefore, a solution of EB has been used as a spectral probe since it does not emit in the buffer solution due to probable quenching of its emission by the solvent.²⁸ However, intense emission is observed when EB strongly intercalates with the adjacent DNA base pairs. But a decrease in emission intensity results from the displacement of EB by a quencher molecule. The extent of emission quenching could be used to determine the extent of binding between the metal complex with DNA.²⁸

For all the ligands and Ag(I) complexes, no emission was observed either alone or in the presence of CT-DNA in the buffer. So the binding of complexes with CT-DNA cannot be

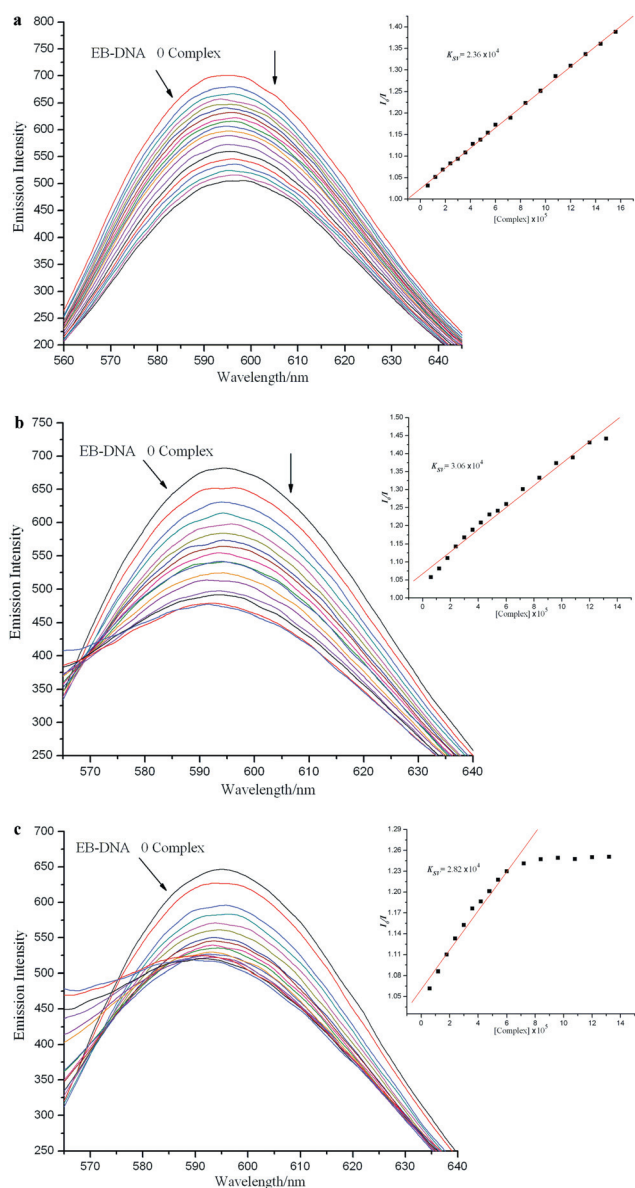


Fig. 11 Fluorescence spectra of the DMF solution of complexes (a) **1**, (b) **2**, and (c) **3** in Tris-HCl buffer upon addition of CT-DNA. $[\text{Complex}] = 3 \times 10^{-5} \text{ M}^{-1}$. Arrow shows the intensity changing upon increasing CT-DNA concentrations. A Stern–Volmer quenching plot of the Ag(I) complexes inserting in their own fluorescence spectra with increasing concentrations of CT-DNA.

directly presented in the emission spectra. Therefore, competitive EB binding studies could be undertaken in order to examine the binding of each complex with DNA. The fluorescence quenching of EB bound to CT-DNA by complexes **1–3** is shown in Fig. 11a–c. The quenching of EB bound to CT-DNA by three Ag(I) complexes are in good agreement with the linear Stern–Volmer equation, which provides further evidence that the Ag(I) complexes bind to DNA and only one type of quenching process occurs. The K_{sv} values of ligands **L**¹–**L**³ were $1.05 \times 10^4 \text{ M}^{-1}$ ($R = 0.99$ for 16 points), $1.67 \times 10^4 \text{ M}^{-1}$ ($R = 0.99$ for 8 points) and $1.40 \times 10^4 \text{ M}^{-1}$ ($R = 0.98$ for 12 points), respectively. The K_{sv} values for complexes **1–3** are $2.36 \times 10^4 \text{ M}^{-1}$ ($R = 0.99$

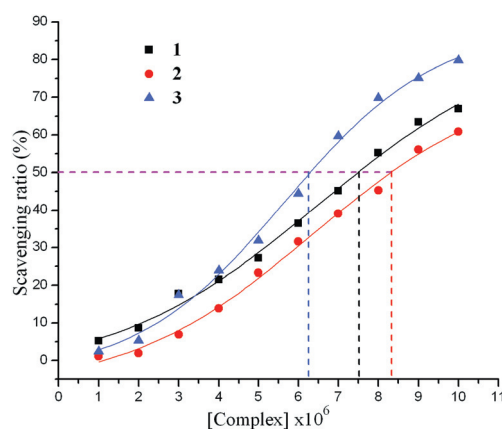


Fig. 12 The inhibitory effect of the three Ag(I) complexes on OH^\cdot radicals; the suppression ratio increases with increasing concentration of the test compound.

for 16 points), $3.06 \times 10^4 \text{ M}^{-1}$ ($R = 0.99$ for 16 points) and $2.85 \times 10^4 \text{ M}^{-1}$ ($R = 0.98$ for 11 points), respectively. The Stern–Volmer dynamic quenching constants can also be interpreted as binding affinities of the complexation reactions.²⁹ Consequently, for three ligands, the values of K_{sv} are very close, which means that they have proximate binding affinity with DNA. However, the values of K_{sv} present the order $2 > 3 > 1$ for complexes, which indicate the abilities of displacement of EtBr from EtBr–DNA systems by compounds and the binding affinities between compounds and DNA, which is consistent with the previous conclusions.

2.4. Hydroxyl radical scavenging activity

Since the ligands and Ag(I) complexes exhibit reasonable DNA-binding affinity, it was considered worthwhile to study other potential aspects, such as antioxidant and antiradical activity. It is a well-documented fact that some transition metal complexes display significant antioxidant activity¹² and therefore we undertook a systematic investigation on the antioxidant potential of free ligands and Ag(I) complexes against OH^\cdot radicals with respect to different concentrations of the test compounds.

We compared the abilities of several present compounds to scavenge hydroxyl radicals with those of the well-known natural antioxidants mannitol and vitamin C, using the same method as reported in a previous paper.³⁰ The 50% inhibitory concentration (IC_{50}) value of mannitol and vitamin C are about 9.6×10^{-3} and $8.7 \times 10^{-3} \text{ M}^{-1}$, respectively. According to the antioxidant experiments, the IC_{50} values of complexes **1**, **2** and **3** are $7.52 \times 10^{-6} \text{ M}^{-1}$, $8.34 \times 10^{-6} \text{ M}^{-1}$ and $6.25 \times 10^{-6} \text{ M}^{-1}$, respectively (Fig. 12), which implies that the three Ag(I) complexes exhibit better scavenging activity than mannitol and vitamin C. It can be concluded that a much less or no scavenging activity was exhibited by the ligands when compared to that of Ag(I) complexes which is due to the chelation of ligand with the central metal atom.³⁰ The lower IC_{50} values observed in antioxidant assays did demonstrate that the three Ag(I) complexes have a strong potential to be applied as scavengers to eliminate radicals.

3. Conclusions

Three V-shaped bis-benzimidazole ligands and their silver(I) complexes have been synthesized and characterized. In complex **1**, the coordination geometry around the central Ag(I) atom is T-shaped owing to the strong interactions between the two Ag(I) atoms themselves. The cation of complex **2** makes up a centrosymmetric dinuclear pore canal structure *via* two ligands coordinated to two Ag(I) atoms. The geometric structure of complex **3** displays an eight-shaped geometry. The experimental results of DNA-binding of the Ag(I) complexes suggest that the three ligands and Ag(I) complexes bind to DNA in an intercalation mode, which is due to the large planar aromatic rings, hydrogen bonds and $\pi\cdots\pi$ stacking interactions that facilitate them intercalating into the base pairs of double helical DNA. The DNA-binding affinities of these three complexes follow the order **2** > **3** > **1**. Moreover, the three Ag(I) complexes also exhibit the effective scavenging of hydroxyl radicals. Information obtained from this study will be helpful to the understanding of the mechanism of interactions with DNA, and should be useful in the development of potential probes of DNA structure and conformation and new therapeutic reagents for some diseases.

4. Experimental

Caution: Although no problems were encountered in this work, transition metal picrate salts are potentially explosive and should thus be prepared in small quantities and handled with care.

4.1. General methods

All chemicals and solvents were reagent grade and were used without further purification. The C, H and N elemental analyses were determined using a Carlo Erba 1106 elemental analyzer. Electrolytic conductance measurements were made with a DDS-307 type conductivity bridge using 3×10^{-3} mol L⁻¹ solutions in DMF at room temperature. The IR spectra were recorded in the 4000–400 cm⁻¹ region with a Nicolet FT-VERTEX 70 spectrometer using KBr pellets. Electronic spectra were taken on a Lab-Tech UV Bluestar spectrophotometer. The fluorescence spectra were recorded on a LS-45 spectrofluorophotometer. The absorbance was measured with a Spectrumlab 722sp spectrophotometer at room temperature. ¹H NMR spectra were recorded on a Varian VR300-MHz spectrometer with TMS as an internal standard.

Calf thymus DNA (CT-DNA) and ethidium bromide (EB) were purchased from Sigma. All chemicals used were of analytical grade. The solution of CT-DNA gave a ratio of UV absorbance at 260 and 280 nm, A_{260}/A_{280} , of 1.8–1.9, indicating that the DNA was sufficiently free of protein.^{18b,e} The stock solution of DNA (2.5×10^{-3} M) was prepared in 5 mM Tris-HCl/50 mM NaCl buffer solution (pH = 7.2, stored at 4 °C and used within 4 days). The CT-DNA concentration per nucleotide was determined spectrophotometrically by employing an extinction coefficient of 6600 M⁻¹ cm⁻¹ at 260 nm.³¹ The stock solution of ligands and Ag(I) complexes were dissolved in DMF at the concentration 3×10^{-3} M.

4.2. Synthesis of the ligands

Synthesis of L¹. L¹ was synthesized following a slight modification of the procedure in ref. 32. The conventional solid-phase reaction reported in ref. 32 was replaced by the ethylene glycol solution method. Refluxing for 24 h, the resulting solution was poured into ice water, a pale yellow precipitate was obtained, left to rest for 30 min then filtered, and recrystallized from ethanol to give L¹. (Yield: 74%; m.p.: 104–106 °C. Found (%): C, 75.31; H, 5.53; N, 19.15. Calcd (%) for C₂₃H₂₁N₅: C, 75.18; H, 5.76; N, 19.06. ¹H NMR (DMSO-d₆ 400 MHz) δ /ppm: 3.47 (m, 2H, $-CH_2-Ar$), 3.85 (s, 4H, $-CH_2$ -benzimidazol), 7.20 (m, 5H, H-benzene ring), 7.35–7.62 (m, 8H, H-benzimidazol ring). Λ_m (DMF, 297 K): 1.45 S cm² mol⁻¹. UV-vis (λ , nm): 278, 284. FT-IR (KBr ν /cm⁻¹): 743, $\nu(o-Ar)$; 1271, $\nu(C-N)$; 1438, $\nu(C=N)$, 1622, $\nu(C=C)$.

Synthesis of L². 7.34 g (20 mmol) L¹ and 1.56 g (40 mmol) potassium were added in tetrahydrofuran (150 mL) and the solution was refluxed on a water bath for 4 h with stirring. Then, 5.68 g (40 mmol) iodomethane was added to this solution. With the dropping of iodomethane, the solution gradually becomes cream yellow. After that, the resulting solution was concentrated and cooled until a pale yellow solid separated out, then the pale yellow precipitate was filtered, washed with excess water, and recrystallized from ethanol to give L². Yield: 4.85 g (58%); m.p.: 185–186 °C. Found (%): C, 75.69; H, 6.54; N, 17.77. Calcd (%) for C₂₅H₂₅N₅: C, 75.92; H, 6.37; N, 17.71. ¹H NMR (DMSO-d₆ 400 MHz) δ /ppm: 3.45–3.62 (s, 6H, $-CH_3$), 3.70 (m, 4H, $-CH_2-Ar$), 3.90 (m, 4H, $-CH_2$ -benzimidazol), 7.23 (m, 5H, H-benzene ring), 7.27–7.61 (m, 8H, H-benzimidazol ring). UV-vis (λ , nm): 279, 287. IR (KBr ν /cm⁻¹): 750, $\nu(o-Ar)$; 1230, $\nu(C-N)$; 1475, $\nu(C=N)$; 1616, $\nu(C=C)$.

Synthesis of L³. L³ was prepared by a similar procedure as for L², except using 6.84 g (40 mmol) benzyl bromide instead of iodomethane. (Yield: 5.56 g, 61%); m.p.: 156–158 °C. Found (%): C, 81.02; H, 6.26; N, 12.69. Calcd (%) for C₃₇H₃₃N₅: C, 81.14; H, 6.07; N, 12.79. ¹H NMR (DMSO-d₆ 400 MHz) δ /ppm: 3.77 (m, 2H, $-CH_2-Ar$), 3.85 (s, 4H, $-CH_2$ -benzimidazol), 5.27 (m, 4H, $-CH_2-Ar$), 6.89 (m, 5H, H-benzene ring), 7.19–7.26 (s, 10H, H-benzene ring), 7.42–7.64 (m, 8H, H-benzimidazol ring). Λ_m (DMF, 297 K): 4.16 S cm² mol⁻¹. UV-vis (λ , nm): 279, 287. FT-IR (KBr ν /cm⁻¹): 740, $\nu(o-Ar)$; 1286, $\nu(C-N)$; 1464, $\nu(C=N)$, 1612, $\nu(C=C)$.

4.3. Preparation of complexes

The three complexes were prepared by a similar procedure. To a stirred solution of ligand (0.50 mmol; L¹, 183.5 mg; L², 197.5 mg; L³, 273.5 mg) in hot EtOH (10 mL) was added Ag (pic) (170.0 mg, 0.50 mmol) in mixed MeCN–EtOH solution (2 mL; MeCN–EtOH = 3:1). A yellow crystalline product formed rapidly. The precipitate was filtered off, washed with EtOH and absolute Et₂O, and dried *in vacuo*. The dried precipitate was dissolved in acetonitrile to form a yellow solution into which Et₂O was allowed to diffuse at room temperature. Crystals suitable for X-ray measurement were obtained after several weeks.¹¹

Table 1 Crystal and structure refinement data for complexes **1**, **2** and **3**

Complex	1	2	3
Empirical formula	C ₅₈ H ₄₆ Ag ₂ N ₁₆ O ₁₄	C ₆₈ H ₆₈ Ag ₂ N ₁₈ O ₁₆	C ₄₃ H ₃₅ AgN ₈ O ₇
Molecular weight	1406.85	1609.14	883.66
Crystal system	Triclinic	Monoclinic	Triclinic
Space group	<i>P</i> $\bar{1}$	<i>P2</i> ₁ / <i>c</i>	<i>P</i> $\bar{1}$
<i>a</i> (Å)	8.6538(12)	12.4814(17)	9.725(9)
<i>b</i> (Å)	13.3823(19)	18.698(3)	14.739(14)
<i>c</i> (Å)	13.6460(19)	16.038(2)	16.516(16)
α (°)	67.8070(10)	90	65.574(9)
β (°)	79.521(2)	111.682(2)	81.098(9)
γ (°)	88.5650(10)	90	77.451(9)
<i>V</i> (Å ³)	1437.2(3)	3477.9(8)	2098(3)
<i>Z</i> , <i>D</i> _c (mg m ⁻³)	1, 1.625	2, 1.537	2, 1.399
μ (mm ⁻¹)	0.764	0.645	0.540
<i>F</i> (000)	712	1648	904
θ range for data collection (°)	2.64–26.00	2.09–25.00	2.15–25.50
Crystal size (mm)	0.32 × 0.28 × 0.24	0.34 × 0.30 × 0.24	0.34 × 0.31 × 0.26
Limiting indices, <i>h k l</i>	–10 to 10 –16 to 16 –16 to 16	–12 to 14 –22 to 21 –19 to 18	–11 to 11 –17 to 17 –19 to 19
Reflections collected	10 975	17 486	15 185
Unique reflections	5573	6107	7677
<i>R</i> _{int}	0.0197	0.0301	0.0234
Data/restraints/parameters	5573/0/406	6107/0/473	7677/14/532
Goodness-of-fit on <i>F</i> ²	1.015	1.045	1.098
<i>R</i> ₁ / <i>wR</i> ₂ [<i>I</i> > 2 σ (<i>I</i>)]	0.0384/0.0786	0.0374/0.0876	0.0527/0.1492
<i>R</i> ₁ / <i>wR</i> ₂ (all data)	0.0543/0.0858	0.0544/0.0954	0.0781/0.1737
Largest diff. peak, hole (e Å ⁻³)	0.577, –0.526	0.703, –0.482	1.705, –0.463

1, (Yield: 235.5 mg, 67%). Found (%): C, 40.29; H, 2.56; N, 14.74. Calcd (%) for C₅₈H₄₆Ag₂N₁₆O₁₄: C, 40.45; H, 2.42; N, 14.82. *A*_m (DMF, 297 K): 90.54 S cm² mol⁻¹. UV-vis (λ , nm): 275, 282, 381. FT-IR (KBr ν /cm⁻¹): 736, ν (*o*-Ar); 1269, ν (C–N); 1363, ν (O–N–O); 1454, ν (C=N), 1616, ν (C=C).

2, (Yield: 257.4 mg, 64%). Found (%): C, 42.32; H, 3.04; N, 14.81. Calcd (%) for C₆₈H₆₈Ag₂N₁₈O₁₆: C, 42.13 H, 3.18; N, 14.74. *A*_m (DMF, 297 K): 77.87 S cm² mol⁻¹. UV-vis (λ , nm): 277, 284, 381. FT-IR (KBr ν /cm⁻¹): 748, ν (*o*-Ar); 1259, ν (C–N); 1365, ν (O–N–O); 1442, ν (C=N), 1629, ν (C=C).

3, (Yield: 265.7 mg, 75%). Found (%): C, 58.21; H, 3.92; N, 12.83. Calcd (%) for C₄₃H₃₅AgN₈O₇: C, 58.45 H, 3.99; N, 12.68. *A*_m (DMF, 297 K): 55.98 S cm² mol⁻¹. UV-vis (λ , nm): 276, 284, 381. FT-IR (KBr ν /cm⁻¹): 742, ν (*o*-Ar); 1264, ν (C–N); 1365, ν (O–N–O); 1449, ν (C=N), 1622, ν (C=C).

4.4. X-ray crystallography

Suitable single crystals were mounted on a glass fiber, and the intensity data were collected on a Bruker Smart CCD diffractometer with graphite-monochromated Mo-K α radiation (λ = 0.71073 Å) at 296 K. Data reduction and cell refinement were performed using the SMART and SAINT programs. The absorption corrections are carried out by the empirical method. The structure was solved by direct methods and refined by full-matrix least-squares against *F*² of data using SHELXTL software.³³ All H atoms were found in difference electron maps and were subsequently refined in a riding-model approximation with C–H distances ranging from 0.93 to 0.97 Å and *U*_{iso}(H) = 1.2 or 1.5 *U*_{eq}(C_{methyl}). Basic crystal data, descriptions of the diffraction experiment, and details of the structure refinement are given in

Table 2 Selected bond distances (Å) and angles (°) for complexes **1–3**

Complex 1			
Ag–N(1)	2.1088(16)	N(3)–Ag#1 ^a	2.1038(15)
Ag–N(3)#1 ^a	2.1038(15)		
C(9)–O(1)–C(8)	112.12(14)	C(1)–N(1)–Ag	123.11(13)
N(3)#1–Ag–N(1) ^a	169.94(6)	C(7)–N(1)–Ag	129.50(13)
C(10)–N(3)–Ag#1 ^a	126.54(13)	C(16)–N(3)–Ag#1 ^a	126.57(13)
Complex 2			
Ag(1)–N(1)	2.124(3)	Ag(1)–N(7)	2.134(3)
Ag(1)–Ag(2)	2.9973(4)	Ag(2)–N(3)	2.117(3)
Ag(2)–N(5)	2.134(3)	Ag(2)–O(3)	2.526(3)
N(1)–Ag(1)–N(7)	177.90(12)	N(1)–Ag(1)–Ag(2)	90.66(8)
N(7)–Ag(1)–Ag(2)	89.32(8)	N(3)–Ag(2)–N(5)	164.91(12)
N(3)–Ag(2)–O(3)	104.34(12)	N(5)–Ag(2)–O(3)	90.63(12)
N(3)–Ag(2)–Ag(1)	79.32(8)	N(5)–Ag(2)–Ag(1)	89.23(8)
O(3)–Ag(2)–Ag(1)	132.51(7)	C(41)–O(3)–Ag(2)	141.5(3)
Complex 3			
Ag(1)–N(3)	2.166(5)	Ag(1)–N(7)	2.174(5)
Ag(1)–O(12)	2.551(4)	Ag(1)–Ag(2)	3.1365(7)
Ag(2)–N(1)	2.138(5)	Ag(2)–N(5)	2.145(5)
N(3)–Ag(1)–N(7)	163.5(2)	N(3)–Ag(1)–O(12)	103.15(17)
N(7)–Ag(1)–O(12)	85.46(18)	N(3)–Ag(1)–Ag(2)	86.16(13)
N(7)–Ag(1)–Ag(2)	88.14(14)	O(12)–Ag(1)–Ag(2)	166.26(10)
N(1)–Ag(2)–N(5)	167.08(19)	N(1)–Ag(2)–Ag(1)	83.42(14)
N(5)–Ag(2)–Ag(1)	88.90(14)	C(68)–O(12)–Ag(1)	124.3(4)

^a Symmetry transformations used to generate equivalent atoms: #1 1 – *x*, 1 – *y*, –*z*.

Table 1. Selected bond distances and angles are presented in Table 2.

Crystallographic data for complexes **1–3** have been deposited with the Cambridge Crystallographic Data Centre as supplementary publication. CCDC reference numbers are 831425, 831426 and 831427, respectively.†

4.5. DNA-binding experiments

Viscosity titration measurements. Viscosity experiments were conducted on an Ubbelohde viscometer, immersed in a water bath maintained at 25.0 ± 0.1 °C. The flow time was measured with a digital stopwatch and each sample was tested three times to get an average calculated time. Titrations were performed for the complexes (3–30 μM), and each compound was introduced into CT-DNA solution (42.5 μM) present in the viscometer. Data were presented as $(\eta/\eta_0)^{1/3}$ versus the ratio of the concentration of the compound to CT-DNA, where η is the viscosity of CT-DNA in the presence of the compound and η_0 is the viscosity of CT-DNA alone. Viscosity values were calculated from the observed flow time of CT-DNA-containing solutions corrected from the flow time of buffer alone (t_0), $\eta = (t - t_0)^{3.4}$

Electronic absorption titration. All spectrophotometric measurements were performed in thermostated quartz sample cells at 25 °C. Solutions for analysis were prepared by dilution of stock solutions immediately before the experiments. Spectrophotometer slit widths were kept at 1 nm for absorption spectroscopy and 5/5 nm for emission spectroscopy. Electronic absorption titration experiments were performed by maintaining the concentration of the test compounds (ligands/complexes) as constant (30 μM) while gradually increasing the concentration of CT-DNA. To obtain the absorption spectra, the required amount of CT-DNA was added to both compound solution and the reference solution to eliminate the absorbance of CT-DNA itself.³⁵ Each sample solution was scanned in the range of 190–500 nm, and the mixture was allowed to equilibrate for 5 min before the spectra were recorded. From the absorption titration data, the binding constant (K_b) was determined using the equation:²⁴

$$[\text{DNA}]/(\varepsilon_a - \varepsilon_f) = [\text{DNA}]/(\varepsilon_b - \varepsilon_f) + 1/K_b(\varepsilon_b - \varepsilon_f)$$

where [DNA] is the concentration of CT-DNA in base pairs, ε_a corresponds to the extinction coefficient observed ($A_{\text{obsd}}/[\text{M}]$), ε_f corresponds to the extinction coefficient of the free compound, ε_b is the extinction coefficient of the compound when fully bound to CT-DNA, and K_b is the intrinsic binding constant. The ratio of slope to intercept in the plot of $[\text{DNA}]/(\varepsilon_a - \varepsilon_f)$ versus [DNA] gave the value of K_b .

Competitive binding with ethidium bromide. EB emits intense fluorescence in the presence of CT-DNA, due to its strong intercalation between the adjacent CT-DNA base pairs. It was previously reported that the enhanced fluorescence can be quenched by the addition of a second molecule.³⁶ The extent of fluorescence quenching of EB bound to CT-DNA can be used to determine the extent of binding between the second molecule and CT-DNA. The effect of each complex with the DNA–EB complex was studied by adding a certain amount of a solution of the complex step by step into the buffer solution of the DNA–EB complex.³⁷ The fluorescence spectra of EB were measured using an excitation wavelength of 520 nm, and the emission range was set between 550 and 750 nm. The influence of the addition of each compound to the DNA–EB complex solution has been obtained by recording the variation of the fluorescence emission spectra. The spectra were analyzed according to the classical Stern–Volmer equation:³⁸

$$I_0/I = 1 + K_{\text{sv}}[Q]$$

where I_0 and I are the fluorescence intensities at 599 nm in the absence and presence of the quencher, respectively, K_{sv} is the linear Stern–Volmer quenching constant, and $[Q]$ is the concentration of the quencher. In these experiments $[\text{CT-DNA}] = 2.5 \times 10^{-3}$ mol L⁻¹, $[\text{EB}] = 2.2 \times 10^{-3}$ mol L⁻¹.

4.6. Hydroxyl radical scavenger measurements

Hydroxyl radicals were generated in aqueous media through the Fenton-type reaction.³⁹ The aliquots of reaction mixture (3 mL) contained 1.0 mL of 0.10 mmol aqueous safranin, 1 mL of 1.0 mmol aqueous EDTA-Fe(II), 1 mL of 3% aqueous H₂O₂, and a series of quantitative microadditions of solutions of the test compound. A sample without the tested compound was used as the control. The reaction mixtures were incubated at 37 °C for 30 min in a water bath. The absorbance was then measured at 520 nm. All the tests were run in triplicate and are expressed as the mean and standard deviation (SD).⁴⁰ The scavenging effect for OH· was calculated from the following expression:

$$\text{Scavenging ratio (\%)} = [(A_i - A_0)/(A_c - A_0)] \times 100\%$$

where A_i = absorbance in the presence of the test compound; A_0 = absorbance of the blank in the absence of the test compound; A_c = absorbance in the absence of the test compound, EDTA-Fe(II) and H₂O₂.

Acknowledgements

The authors acknowledge the financial support and grant from ‘Qing Lan’ Talent Engineering Funds by Lanzhou Jiaotong University. The grant from ‘Long Yuan Qing Nian’ of Gansu Province also is acknowledged.

References

- (a) A. N. Khlobystov, A. J. Blake, N. R. Champness, D. A. Lemenovskii, A. G. Majouga, N. V. Zyk and M. Schröder, *Coord. Chem. Rev.*, 2001, **222**, 155; (b) C.-L. Chen, B.-S. Kang and C.-Y. Su, *Aust. J. Chem.*, 2006, **59**, 3; (c) S. M. Gortez and R. G. Rapti, *Coord. Chem. Rev.*, 1998, **169**, 363; (d) S.-L. Zheng, M.-L. Tong and X.-M. Chen, *Coord. Chem. Rev.*, 2003, **246**, 185; (e) A. J. Blake, N. R. Champness, P. Hubberstey, W.-S. Li, M. A. Withersby and M. Schröder, *Coord. Chem. Rev.*, 1999, **183**, 117; (f) M. Munakata, L. P. Wu and G.-L. Ning, *Coord. Chem. Rev.*, 2000, **198**, 171; (g) S. L. James, X.-L. Xu and R. V. Law, *Macromol. Symp.*, 2003, **196**, 187; (h) M. O. Awaleh, A. Badia, F. Brisse and X. H. Bu, *Inorg. Chem.*, 2006, **45**, 1560.
- (a) C. A. Grapperhaus, M. Li and M. S. Mashuta, *Chem. Commun.*, 2002, 1792; (b) P. J. Steel and C. J. Sumbly, *Chem. Commun.*, 2002, 322; (c) M. J. Hannon, C. L. Painting, E. A. Plummer, L. J. Childs and N. W. Alcock, *Chem.–Eur. J.*, 2002, **8**, 2225; (d) Y.-B. Dong, H.-Q. Zhang, J.-P. Ma, R.-Q. Huang and C.-Y. Su, *Cryst. Growth Des.*, 2005, **5**, 1857; (e) X.-P. Li, J.-Y. Zhang, M. Pan, S.-R. Zheng, Y. Liu and C.-Y. Su, *Inorg. Chem.*, 2007, **46**, 4617; (f) X.-H. Bu, Y.-B. Xie, J.-R. Li and R.-H. Zhang, *Inorg. Chem.*, 2003, **42**, 7422.
- (a) C. B. Aakeröy, D. John, M. S. Michelle and F. U. Joaquin, *Dalton Trans.*, 2005, 2462; (b) B. Moulton and M. J. Zaworotko, *Chem. Rev.*, 2001, **101**, 1629; (c) O. R. Evans and W.-B. Lin, *Acc. Chem. Res.*, 2002, **35**, 511; (d) S. M. Kil and P. S. Myunghyun, *J. Am. Chem. Soc.*, 2000, **122**, 6834; (e) A. Y. Robin and K. M. Fromm, *Coord. Chem. Rev.*, 2006, **250**, 2127.
- (a) J. Reedijk, in *Heterocyclic Nitrogen-Donor Ligands Comprehensive Coordination Chemistry*, ed. G. Wilkinson, R. D. Gillard and J. A. McCleverty, Pergamon Press, Oxford, 1987, vol. 2 (and references therein), p. 73; (b) D. A. House, in: *Ammonia and Amines*.

- Comprehensive Coordination Chemistry*, ed. G. Wilkinson, R. D. Gillard and J. A. McCleverty, Pergamon Press, Oxford, 1987, vol. 2 (and references therein), p. 23.
- 5 (a) F. Grob, A. Müller-Hartmann and H. Vahrenkamp, *Eur. J. Inorg. Chem.*, 2000, **11**, 2363; (b) W. L. Driessen, R. A. G. Graaf, F. J. Pavevliet, J. Reedijk and R. M. de Vos, *Inorg. Chim. Acta*, 1994, **216**, 43; (c) S.-X. Wang, Q.-H. Luo, X.-M. Wang, L.-F. Wang and K.-B. Yu, *J. Chem. Soc., Dalton Trans.*, 1995, 2045; (d) H. Adams, N. A. Bailey, J. D. Crane, D. E. Fenton, J. M. Latour and J. M. Williams, *J. Chem. Soc., Dalton Trans.*, 1990, 1727.
 - 6 (a) N. T. A. Ghani and A. M. Mansour, *Inorg. Chim. Acta*, 2011, **373**, 249; (b) S.-X. Wang, S.-Y. Yu and Q.-H. Luo, *Transition Met. Chem.*, 1994, **19**, 205.
 - 7 (a) D. A. Horton, G. T. Bourne and M. L. Smythe, *Chem. Rev.*, 2003, **103**, 893; (b) J. J. Perry IV, J. A. Perman and M. J. Zaworotko, *Chem. Soc. Rev.*, 2009, **38**, 1400; (c) M. G. Moeller, L. F. Campo, A. Brandelli and V. Stefani, *J. Photochem. Photobiol., A*, 2002, **149**, 217; (d) J. M. Grevy, F. Tellez, S. Bernés, H. Nöth, R. Contreras and N. Barba-Behrens, *Inorg. Chim. Acta*, 2002, **339**, 532; (e) J.-P. Zhang, X.-C. Huang and X.-M. Chen, *Chem. Soc. Rev.*, 2009, **38**, 2385.
 - 8 (a) R. R. Tidwell, S. K. Jones, N. A. Naiman, L. C. Berger, W. B. Brake, C. C. Dykstra and J. E. Hall, *Antimicrob. Agents Chemother.*, 1993, **37**, 1713; (b) J. Mann, A. Baron, Y. Opoku-Boahen, E. Johansson, G. Parkinson, L. R. Kelland and S. Neidle, *J. Med. Chem.*, 2001, **44**, 138; (c) J.-Y. Xu, Y. Zeng, Q. Ran, Z. Wei, Y. Bi, Q.-H. He, Q.-J. Wang, S. Hu, J. Zhang, M.-Y. Tang, W.-Y. Hua and X.-M. Wu, *Bioorg. Med. Chem. Lett.*, 2007, **17**, 2921; (d) P. D. Patel, M. R. Patel, N. Kaushik-Basu and T. T. Talele, *J. Chem. Inf. Model.*, 2008, **48**, 42; (e) E. E. Alberto, L. L. Rossato, S. H. Alves, D. Alves and A. L. Braga, *Org. Biomol. Chem.*, 2011, **9**, 1001; (f) S. Estrada-Soto, R. Villalobos-Molina, F. Aguirre-Crespo, J. Vergara-Galicia, H. Oreno-Diaz, M. Torres-Piedra and G. Navarrete-Vázquez, *Life Sci.*, 2006, **79**, 430; (g) V. Rajendiran, M. Murali, E. Suresh, S. Sinha, K. Somasundaram and M. Palaniandavar, *Dalton Trans.*, 2008, 148.
 - 9 (a) S. Santra and S. K. Dogra, *J. Mol. Struct.*, 1999, **476**, 223; (b) T. M. Aminabhavi, N. S. Biradar, S. B. Patil and D. E. Hoffman, *Inorg. Chim. Acta*, 1986, **125**, 125.
 - 10 (a) C. J. Matthews, V. Broughton, G. Bernardinelli, X. Melich, G. Brand, A. C. Willis and A. F. Williams, *New J. Chem.*, 2003, **27**, 354; (b) D. Moon, M. S. Lah, R. E. D. Sesto and J. S. Miller, *Inorg. Chem.*, 2002, **41**, 4708; (c) B. S. Hammes, M. T. Kieber-Emmons, R. Sommer and A. L. Rheingold, *Inorg. Chem.*, 2002, **41**, 1351.
 - 11 (a) H.-L. Wu, X.-C. Huang, J.-K. Yuan, F. Kou, F. Jia, B. Liu and K.-T. Wang, *Eur. J. Med. Chem.*, 2010, **45**, 5323; (b) H.-L. Wu, K. Li, T. Sun, F. Kou, F. Jia, J.-K. Yuan, B. Liu and B.-L. Qi, *Transition Met. Chem.*, 2010, **36**, 21; (c) H.-L. Wu, R.-R. Yun, K.-T. Wang, K. Li, X.-C. Huang, T. Sun and Y.-Y. Wang, *J. Coord. Chem.*, 2010, **63**, 243; (d) H.-L. Wu, X.-C. Huang, J.-K. Yuan, K. Li, J. Ding, R.-R. Yun, W.-K. Dong and X.-Y. Fan, *J. Coord. Chem.*, 2009, **62**, 3446; (e) H.-L. Wu, R.-R. Yun, K.-T. Wang, K. Li, X.-C. Huang and T. Sun, *Z. Anorg. Allg. Chem.*, 2010, **636**, 629; (f) H.-L. Wu, J.-K. Yuan, Y. Bai, F. Jia, B. Liu, F. Kou and J. Kong, *Transition Met. Chem.*, 2011, **36**, 819; (g) H.-L. Wu, J.-K. Yuan, Y. Bai, G.-L. Pan, H. Wang and X.-B. Shu, *J. Photochem. Photobiol., B*, 2012, **107**, 65.
 - 12 (a) S. B. Bukhari, S. Memon, M. Mahroof-Tahir and M. I. Bhanter, *Spectrochim. Acta, A. Mol. Biomol. Spectrosc.*, 2009, **7**, 11901; (b) I. B. Afanasev, E. A. Ostrakhovitch, E. V. Mikhallchi, G. A. Ibragimova and L. G. Korkina, *Biochem. Pharmacol.*, 2001, **61**, 677; (c) F. V. Botelho, J. I. Alvarez-Leite, V. S. Lemos, A. M. C. Pimenta, H. D. R. Calado, T. Matencio, C. T. Miranda and E. C. Pereira-Maia, *J. Inorg. Biochem.*, 2007, **101**, 935; (d) Q. Wang, Z.-Y. Yang, G.-F. Qi and D.-D. Qin, *Eur. J. Med. Chem.*, 2009, **44**, 2425.
 - 13 W. J. Geary, *Coord. Chem. Rev.*, 1971, **7**, 81.
 - 14 (a) T. J. Lane, I. Nakagawa, J. L. Walter and A. J. Kandathil, *Inorg. Chem.*, 1962, **1**, 267; (b) J. S. Richard and R. B. Martin, *Chem. Rev.*, 1974, **74**, 471; (c) E. K. Chec, M. Kubiak, T. Glowiak and J. J. Ziolkowski, *Transition Met. Chem.*, 1998, **23**, 641.
 - 15 T. Fonseca, B. Gigante and T. L. Gilchrist, *Tetrahedron*, 2001, **57**, 1793.
 - 16 (a) K. N. Power, T. L. Hennigar and M. J. Zaworotko, *New J. Chem.*, 1998, **22**, 177; (b) O. M. Yaghi and H. J. Li, *J. Am. Chem. Soc.*, 1996, **118**, 295.
 - 17 C.-L. Chen, C.-Y. Su, Y.-P. Cai, H.-X. Zhang, A.-W. Xu, B.-S. Kang and Z. L. Hans-Conrad, *Inorg. Chem.*, 2003, **42**, 3738.
 - 18 (a) Y.-C. Liu and Z.-Y. Yang, *Eur. J. Med. Chem.*, 2009, **44**, 5080; (b) S. Satyanarayana, J. C. Dabrowiak and J. B. Chaires, *Biochemistry*, 1993, **32**, 2573; (c) D. S. Sigman, A. Mazumder and D. M. Perrin, *Chem. Rev.*, 1993, **93**, 2295; (d) Y. Wang, Z.-Y. Yang, Q. Wang, Q.-K. Cai and K.-B. Yu, *J. Organomet. Chem.*, 2005, **690**, 4557; (e) S. Satyanarayana, J. C. Dabrowiak and J. B. Chaires, *Biochemistry*, 1992, **31**, 9319.
 - 19 (a) D. Suh and J. B. Chaires, *Bioorg. Med. Chem.*, 1995, **3**, 723; (b) R. Palchadhuri and P. J. Hergenrother, *Curr. Opin. Biotechnol.*, 2007, **18**, 497.
 - 20 B.-D. Wang, Z.-Y. Yang, P. Crewdson and D.-Q. Wang, *J. Inorg. Biochem.*, 2007, **101**, 1492.
 - 21 (a) C. Metcalfe and J. A. Thomas, *Chem. Soc. Rev.*, 2003, **32**, 215; (b) I. Ortman, C. Moucheron and A. K. D. Mesmaeker, *Coord. Chem. Rev.*, 1998, **168**, 233; (c) H. Chao and L.-N. Ji, *Bioinorg. Chem. Appl.*, 2005, **3**, 15; (d) B. Peng, H. Chao, B. Sun, H. Li, F. Gao and L.-N. Ji, *J. Inorg. Biochem.*, 2007, **101**, 404.
 - 22 (a) S. Yellappa, J. Seetharamappa, L. M. Rogers, R. Chitta, R. P. Singhal and F. D'Souza, *Bioconjugate Chem.*, 2006, **17**, 1418; (b) M. Shakir, M. Azam, M. F. Ullah and S. M. Hadi, *J. Photochem. Photobiol., B*, 2011, **104**, 449.
 - 23 (a) J. K. Barton, A. T. Danishefsky and J. M. Goldberg, *J. Am. Chem. Soc.*, 1984, **106**, 2172; (b) H.-L. Lu, J.-J. Liang, Z.-Z. Zeng, P.-X. Xi, X.-H. Liu, F.-J. Chen and Z.-H. Xu, *Transition Met. Chem.*, 2007, **32**, 564.
 - 24 (a) C. Behrens, N. Harrit and P. E. Nielsen, *Bioconjugate Chem.*, 2001, **12**, 1021; (b) S. Frau, J. Bernadou and B. Meunier, *Bioconjugate Chem.*, 1997, **8**, 222.
 - 25 A. M. Pyle, J. P. Rehmann, R. Meshoyrer, C. V. Kumar, N. J. Turro and J. K. Barton, *J. Am. Chem. Soc.*, 1989, **111**, 3051.
 - 26 S. Nafisi, A. A. Saboury, N. Keramat, J. F. Neault and H. A. Tajmir-Riahi, *J. Mol. Struct.*, 2007, **827**, 35.
 - 27 J.-Z. Wu, B.-H. Ye, L. Wang, L.-N. Ji, J.-Y. Zhou, R.-H. Li and Z.-Y. Zhou, *J. Chem. Soc., Dalton Trans.*, 1997, 1395.
 - 28 (a) J. B. LePecq and C. Paoletti, *J. Mol. Biol.*, 1967, **27**, 87; (b) R. Gaura, R. A. Khanb, S. Tabassumb, P. Shahc, M. I. Siddiqic and L. Mishraa, *J. Photochem. Photobiol., A*, 2011, **220**, 145.
 - 29 (a) L. A. Bagatolli, S. C. Kivatinitz and G. D. Fidelio, *J. Pharm. Sci.*, 1996, **85**, 1131; (b) M.-M. Yang, P. Yang and L.-W. Zhang, *Chin. Sci. Bull.*, 1994, **9**, 31.
 - 30 (a) T.-R. Li, Z.-Y. Yang, B.-D. Wang and D.-D. Qin, *Eur. J. Med. Chem.*, 2008, **43**, 1688; (b) J.-I. Ueda, N. Saito, Y. Shimazu and T. Ozawa, *Arch. Biochem. Biophys.*, 1996, **333**, 377.
 - 31 M. F. Reichmann, S. A. Rice, C. A. Thomas and P. Doty, *J. Am. Chem. Soc.*, 1954, **76**, 3047.
 - 32 K. Takahashi, Y. Nishida and S. Kida, *Polyhedron*, 1984, **3**, 113.
 - 33 (a) Bruker, *Smart Saint and Sadabs*, Bruker Axs, Inc, Madison, WI, 2000; (b) G. M. Sheldrick, *SHELXTL*, Siemens Analytical X-ray Instruments, Inc., Madison, Wisconsin, USA, 1996.
 - 34 C.-P. Tan, J. Liu, L.-M. Chen, S. Shi and L.-N. Ji, *J. Inorg. Biochem.*, 2008, **102**, 1644.
 - 35 (a) M. Tian, H. Ihmels and S. Ye, *Org. Biomol. Chem.*, 2012, **10**, 3010; (b) D. S. Raja, N. S. P. Bhuvaneshb and K. Natarajan, *Dalton Trans.*, 2012, **41**, 4365; (c) L.-M. Chen, J. Liu a, J.-C. Chen, C.-P. Tan, S. Shi, K.-C. Zheng and L.-N. Ji, *J. Inorg. Biochem.*, 2008, **102**, 330.
 - 36 (a) A. Wolf, G. H. Shimer and T. Meehan, *Biochemistry*, 1987, **26**, 6392; (b) B. C. Baguley and M. L. Bret, *Biochemistry*, 1984, **23**, 937.
 - 37 A. Tarushi, G. Psomas, C. P. Raptopoulou, V. Psycharis and D. P. Kessissoglou, *Polyhedron*, 2009, **28**, 3272.
 - 38 J. R. Lakowicz and G. Webber, *Biochemistry*, 1973, **12**, 4161.
 - 39 (a) C. C. Winterbourn, *Biochem. J.*, 1981, **198**, 125; (b) C. C. Winterbourn, *Biochem. J.*, 1979, **182**, 625.
 - 40 Z.-Y. Guo, R.-E. Xing, S. Liu, H.-H. Yu, P.-B. Wang, C.-P. Li and P.-C. Li, *Bioorg. Med. Chem. Lett.*, 2005, **15**, 4600.